

# CASA: Bridging the Gap between Policy Improvement and Policy Evaluation with Conflict Averse Policy Iteration

Changnan Xiao<sup>1</sup> Haosen Shi<sup>2</sup> Jiajun Fan<sup>3</sup> Shihong Deng<sup>4</sup> Haiyan Yin<sup>5</sup>

## Abstract

We study the problem of model-free reinforcement learning, which is often solved following the principle of Generalized Policy Iteration (GPI). While GPI is typically an interplay between policy evaluation and policy improvement, most conventional model-free methods assume the independence of the granularity and other details of the GPI steps, despite of the inherent connections between them. In this paper, we present a method that regularizes the inconsistency between policy evaluation and policy improvement, leading to a conflict averse GPI solution with reduced functional approximation error. To this end, we formulate a novel learning paradigm where taking the policy evaluation step is equivalent to some compensation of performing policy improvement, and thus effectively alleviates the gradient conflict between the two GPI steps. We also show that the form of our proposed solution is equivalent to performing entropy-regularized policy improvement and therefore prevents the policy from being trapped into suboptimal solutions. We conduct extensive experiments to evaluate our method on the Arcade Learning Environment (ALE). Empirical results show that our method outperforms several strong baselines in major evaluation domains.

## 1. INTRODUCTION

Model-free reinforcement learning has made many impressive breakthroughs in a wide range of Markov Decision Processes (MDP) (Vinyals et al., 2019; Pedersen, 2019; Badia et al., 2020a). Overall, the methods could be case into two categories, value-based methods such as DQN (Mnih et al., 2015) and Rainbow (Hessel et al., 2017), as well as policy-based methods such as TRPO (Schulman et al.,

2015a), PPO(Schulman et al., 2017) and IMPALA(Espeholt et al., 2018).

Value-based methods learn state-action values and select the action according to these values. The main target of value-based methods is to approximate the fixed point of the Bellman equation through the generalized policy iteration (GPI)(Sutton & Barto, 2018), which generally consists of the policy evaluation and the policy improvement. One characteristic of the value-based methods is that unless a more accurate state-action values is estimated by iterations of the policy evaluation, the policy will not be improved. So the policy improvement of each policy iteration is limited. Previous works equip value-based methods with many appropriate designed structures, achieving a more promising sample efficiency (Wang et al., 2016; Schaul et al., 2015; Kapturowski et al., 2018).

Policy-based methods learn a parameterized policy directly without consulting state-action values. One merit of policy-based methods is that they incorporate a policy improvement phase every training step, suggesting a more greedy use of samples to improve policy than value-based methods. Nevertheless, policy-based methods easily fall into a suboptimal solution, where the entropy of current policy drops to 0 (Haarnoja et al., 2018), and suffer from high variance caused by environment and stochastic policy. The actor-critic methods introduce a value function as the baseline to reduce the variance of the policy gradient (Mnih et al., 2016), but maintain the other characteristics unchanged.

In this paper, we propose CASA, Critic AS an Actor, an innovative combination of the value-based and the policy-based methods. In general, CASA builds on the actor-critic design that estimates state values  $V$ , state-action values  $Q$  and policy  $\pi$  simultaneously. It integrates a consistent path between the policy evaluation and the policy improvement. It guarantees that **i**) the policy evaluation is equivalent to a compensational policy improvement for the function approximation error; **ii**) the policy evaluation regularizes the policy improvement, which means that CASA does not need any entropy regularization to prevent the policy from collapse.

CASA is capable of large scale training. Due to the fact that large scale training needs off-policy learning, we introduce

<sup>1</sup>xiaochangnan@bytedance.com <sup>2</sup>shihaosen98@gmail.com  
<sup>3</sup>fanjj21@mails.tsinghua.edu.cn <sup>4</sup>dengshihong@bytedance.com  
<sup>5</sup>yinhaiyan@outlook.com. Correspondence to: Changnan Xiao <xiaochangnan@bytedance.com>.

Doubly-Robust Trace (DR-Trace), which **i**) exploits doubly-robust estimator to maximally reduce variances (Jiang & Li, 2016), **ii**) guarantees that  $Q$  and  $V$  converge synchronously to  $Q^*$  and  $V^*$  corresponding to the same policy.

Our main contributions are as follows:

- We propose an actor-critic design, which consists of three intriguing perspectives: **(i)** the policy evaluation and the policy improvement avoid a conflict in GPI steps; **(ii)** the policy evaluation compensates function approximation error; **(iii)** the policy evaluation regularizes the policy improvement from collapse.
- We propose DR-Trace, which incorporates Doubly Robust into a large scale training manner, and prove that the convergence of DR-Trace under the design of CASA is guaranteed.
- We present extensive empirical evaluation results to compare our proposed method with several decent model-free reinforcement learning approaches on Arcade Learning Environment (ALE) (Bellemare et al., 2013; Machado et al., 2018). Our method could outperform several strong baseline approaches on 200 million (200M) training scale.

## 2. Preliminary

Consider an infinite-horizon MDP, defined by  $(\mathcal{S}, \mathcal{A}, p, r, \gamma)$ , where  $\mathcal{S}$  is the state space,  $\mathcal{A}$  is the action space,  $p : \mathcal{S} \times \mathcal{A} \times \mathcal{S} \rightarrow [0, 1]$  is the state transition probability function,  $r : \mathcal{S} \times \mathcal{A} \rightarrow \mathbb{R}$  is the reward function, and  $\gamma$  is the discounted factor. Let  $\pi : \mathcal{S} \times \mathcal{A} \rightarrow [0, 1]$  be the policy.

Define state value function  $V^\pi(s_t) = \mathbb{E}[\sum_{k=0}^{\infty} \gamma^k r_{t+k} | s_t]$ , state-action value function  $Q^\pi(s_t, a_t) = \mathbb{E}[\sum_{k=0}^{\infty} \gamma^k r_{t+k} | s_t, a_t]$ , and advantage function  $A^\pi(s_t, a_t) = Q^\pi(s_t, a_t) - V^\pi(s_t)$ . The connection between  $V^\pi$  and  $Q^\pi$  is given by the Bellman equation,

$$\begin{aligned} \mathcal{T}Q^\pi(s_t, a_t) &= \mathbb{E}_p[r_t + \gamma V^\pi(s_{t+1})], \\ V^\pi(s_t) &= \mathbb{E}_\pi[Q^\pi(s_t, a_t)]. \end{aligned}$$

where  $\mathcal{T}$  is the Bellman Operator,  $\mathbb{E}_p$  is shorthand for  $\mathbb{E}_{s_{t+1} \sim p(s_t, a_t)}$  and  $\mathbb{E}_\pi$  is shorthand for  $\mathbb{E}_{a_t \sim \pi(s_t)}$

The objective of reinforcement learning is to

$$\text{maximize } \mathcal{J} = \mathbb{E}_\pi \left[ \sum_{k=0}^{\infty} \gamma^k r_k \right].$$

Value-based methods maximize  $\mathcal{J}$  by estimating the state-action value function  $Q^\pi$ , which can be improved through GPI until converging to the optimal policy. For the estimated state-value function  $Q_\theta$  that approximates  $Q^\pi$ , the policy evaluation is conducted by minimizing  $\mathbb{E}_\pi[(G - Q_\theta)^2]$ ,

where  $G$  is an estimation of  $Q^\pi(s, a)$  and various methods has been proposed (Schulman et al., 2015b; Munos et al., 2016). The policy evaluation can be achieved by applying gradient ascent on the direction of the gradient  $\theta \leftarrow \theta + \eta \mathbb{E}_\pi[(G - Q_\theta) \nabla_\theta Q_\theta]$ , where  $\eta$  is the learning rate. There are various designs to help estimating  $Q$  functions. A refined structure design of  $Q_\theta$  is provided by dueling-DQN (Wang et al., 2016). It estimates  $Q_\theta$  by the summation of the advantage function and the state value function,  $Q_\theta = A_\theta + V_\theta$ . The policy improvement is usually achieved by selecting a series of actions whose corresponding state-action values are much higher.

Policy-based methods maximize  $\mathcal{J}$  directly by optimizing the parameterized policy  $\pi_\theta$  according to the policy gradient theorem (Sutton & Barto, 2018), which gives  $\nabla_\theta \mathcal{J} = \mathbb{E}_\pi[\Psi(s, a) \nabla_\theta \log \pi_\theta(a|s)]$ , where  $\Psi$  is any  $\gamma$ -just function (Schulman et al., 2015b). The vanilla policy gradient theorem uses  $\Psi = G = \sum_{k=0}^{\infty} \gamma^k r_k$ . When  $\Psi$  involves a baseline, it becomes an actor-critic algorithm. (Espeholt et al., 2018) uses  $\Psi(s_t, a_t) = r_t + \gamma V^{\tilde{\pi}}(s_{t+1}) - V(s_t)$  and introduces V-Trace to estimate  $V^{\tilde{\pi}}$ .

(Ghosh et al., 2020) casts policy-based methods as minimizing a divergence measure between two special policies and regards the policy evaluation and the policy improvement as a projection operator and an improvement operator. It points out that an improvement operator compatible with the projection operator may be preferred.

## 3. Methodology

### 3.1. Motivation

In this section, we use  $V_\theta(s)$  to estimate  $V^\pi(s)$ ,  $Q_\theta(s, a)$  to estimate  $Q^\pi(s, a)$  and  $\pi_\theta(\cdot|s)$  to represent the policy, where we always use  $\theta$  to represent the parameters to be optimized. We use **E** to represent the policy evaluation, which gives the ascent direction of the gradient by  $\theta \leftarrow \theta + \eta \mathbb{E}_\pi[(G - Q_\theta) \nabla_\theta Q_\theta]$ . We use **I** to represent the policy improvement. The policy gradient theorem (Sutton & Barto, 2018) shows that  $\nabla_\theta \mathcal{J} = \mathbb{E}_\pi[G \nabla_\theta \log \pi_\theta]$ , so the gradient ascent given by **I** is  $\theta \leftarrow \theta + \eta \mathbb{E}_\pi[G \nabla_\theta \log \pi_\theta]$ .

Let's rethink GPI shown in Figure 1. To get rid of the function approximation error, we assume the approximation function enjoy infinite capacity. Let  $\beta \stackrel{\text{def}}{=} \angle \nabla_\theta Q_\theta, \nabla_\theta \log \pi_\theta >$  be the angle between the gradient ascent directions of **I** and **E**. When  $\nabla_\theta Q_\theta \propto \nabla_\theta \log \pi_\theta$ , the two sides of  $\beta$  meet, so **I** and **E** become parallel and two black arrows (one iteration) are united into one blue arrow (in 1), which means that there is no conflict between the ascent gradient directions of **I** and **E**.

Next, we assume the representation capacity of the approximation function is limited. When the function approxi-

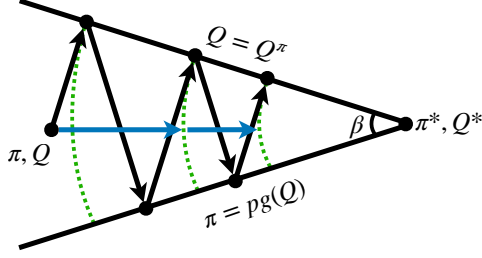


Figure 1. Generalized Policy Iteration (GPI). Different from (Sutton & Barto, 2018), we evaluate  $\pi$  by  $Q$  instead of  $V$ , and improve  $\pi$  by using policy gradient ascent ( $pg$  for brevity) instead of  $\epsilon$ -greedy. The learning process is represented by the black arrows,  $\mathbf{I} \rightarrow \mathbf{E} \rightarrow \dots$ .

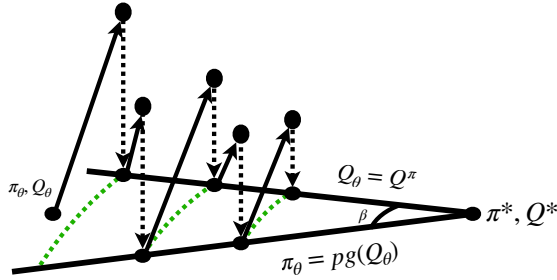


Figure 2. GPI with function approximation. The black arrows represent the policy improvement and the policy evaluation. The dotted arrows represent the projection into the approximated function space. The learning process is represented by the black arrows and dotted arrows,  $\mathbf{I} \rightarrow \mathbf{P}_1 \rightarrow \mathbf{E} \rightarrow \mathbf{P}_E \rightarrow \dots$ .

mation is involved, i.e.  $Q^\pi$  is estimated by  $Q_\theta$  and  $\pi$  is approximated by  $\pi_\theta$ , from the view of operators (Ghosh et al., 2020), each of  $\mathbf{I}$  and  $\mathbf{E}$  can be further decomposed into two operators, as shown in Figure 2. One is to do the policy improvement and the policy evaluation, the other is to project into the restricted function space. We use  $\mathbf{P}_*$  to represent the projection into the approximated function space of  $*$ . When  $\beta > 0$ , GPI with function approximation would involve two projection operators in each iteration, which introduces inevitable approximation error. When  $\beta = 0$ , if the function approximation error is not considered, we find that the gradient conflict between  $\mathbf{I}$  and  $\mathbf{E}$  are totally eliminated. If we consider the limitation of the approximation function, similar to blue arrow in Figure 1, one iteration (two black arrows and two dotted arrows) can be united into one arrow and one dotted arrow, where the gradient conflict is eliminated and the two projection operators are reduced to one additionally.

As stated above, if  $\nabla_\theta Q_\theta \propto \nabla_\theta \log \pi_\theta$  holds, we can expect that both the gradient conflict between the policy improvement and the policy evaluation is eliminated and the function

approximation error is reduced. This motivates us to figure out that *under what condition, the policy improvement and the policy evaluation share the same ascent direction of the gradient, i.e.  $\nabla_\theta Q_\theta \propto \nabla_\theta \log \pi_\theta$ ?*

### 3.2. Formulation

In this section, we use  $V_\theta(s)$  to estimate  $V^\pi(s)$  and  $A_\theta(s, a)$  to estimate  $A^\pi(s, a)$ . Let's start from the Boltzmann policy<sup>1</sup>,  $\pi = \text{softmax}(A_\theta/\tau)$ , where  $A_\theta : \mathcal{S} \rightarrow \mathbb{R}^{|\mathcal{A}|}$  is a parameterized function. We want to find a function  $Q$  satisfying  $\nabla_\theta Q \propto \nabla_\theta \log \pi$  for  $\forall \theta$ .

In order to build the connection between  $Q$  and  $\log \pi$ , we assume that  $Q$  is a function of two parts. The first part is  $A_\theta$  which can completely decide the policy  $\pi$  and the other is  $V_\theta : \mathcal{S} \rightarrow \mathbb{R}$  which is a function only dependent on states. i.e.  $Q_\theta = f(A_\theta, V_\theta)$ .

**Lemma 1.** Let  $g \in C^1(\mathbb{R}^n) : \mathbb{R}^n \rightarrow \mathbb{R}^n$ ,  $f \in C^1(\mathbb{R}^{n+k}) : \mathbb{R}^{n+k} \rightarrow \mathbb{R}^n$ . If  $\nabla_x g(x) = \nabla_x f(x, y)$ , for  $\forall x \in \mathbb{R}^n, y \in \mathbb{R}^k$ , then  $\exists c \in C^1(\mathbb{R}^k) : \mathbb{R}^k \rightarrow \mathbb{R}^n$ , s.t.  $f(x, y) = g(x) + c(y)$ .

*Proof.* See Appendix A, Lemma A.1.  $\square$

Regarding  $x = A_\theta$  to be any vector in  $\mathbb{R}^{|\mathcal{A}|}$ ,  $y = V_\theta$  to be any vector in  $\mathbb{R}^1$ ,  $g = \pi(\cdot|s) = \log \text{softmax}(A_\theta/\tau)$  to be a function of  $A_\theta$  and  $f = Q = f(A_\theta, V_\theta)$  to be a function of  $A_\theta$  and  $V_\theta$  in Lemma 1, let  $\theta = A_\theta$  in  $\nabla_\theta Q \propto \nabla_\theta \log \pi$ , we know

$$\begin{aligned} Q &= f(A_\theta, V_\theta) = \log \text{softmax}(A_\theta/\tau) + c(V_\theta) \\ &\triangleq f_1(A_\theta) + c(V_\theta). \end{aligned}$$

According to the Bellman equation  $\mathbb{E}_\pi[Q] = V_\theta$ , we have

$$\mathbb{E}_\pi[f_1(A_\theta)] = \mathbb{E}_\pi[V_\theta - c(V_\theta)] = V_\theta - c(V_\theta).$$

Since  $\mathbb{E}_\pi[f_1(A_\theta)]$  is not a function of  $V_\theta$ , regarding  $V_\theta$  as a vector in  $\mathbb{R}^1$  and taking  $\partial/\partial V_\theta$  on both sides, we have that  $V_\theta - c(V_\theta)$  is a constant function. Without loss of generality, assume  $V_\theta - c(V_\theta) = 0$ , as we can minus this constant on both sides.

Now we know  $Q = f_1(A_\theta) + V_\theta$ .

Since we will not change  $V_\theta$  when doing the policy improvement, we have  $\partial \log \pi / \partial V_\theta = 0$ . Noting that  $\nabla_\theta Q \propto \nabla_\theta \log \pi \Rightarrow \partial_\theta Q / \partial_\theta V_\theta \propto \partial_\theta \log \pi / \partial_\theta V_\theta = 0$ , we stop the gradient of  $V_\theta$  in  $Q = f_1(A_\theta) + V_\theta$ . Hence, we solve for  $f_1$  s.t.  $\nabla_\theta f_1(A_\theta) \propto \nabla_\theta \log \pi$ .

<sup>1</sup>The Boltzmann policy is a form of policy which is represented by a Boltzmann distribution and  $\text{softmax}(A/\tau) = \exp(A/\tau)/Z$ ,  $Z = \mathbf{1} \cdot \exp(A/\tau)$ , where  $\cdot$  represents inner product and  $\mathbf{1}$  is a vector where every element is 1.

**Lemma 2.** (i) Define  $\pi = \text{softmax}(A/\tau)$ , then  $\nabla \log \pi = (\mathbf{I} - \pi) \frac{\nabla A}{\tau}$ . (ii) Denote  $sg$  to be stop gradient and define  $\bar{A} = A - \mathbb{E}_\pi[A]$ ,  $Q = \bar{A} + sg(V)$ , then  $\nabla Q = (\mathbf{I} - \pi) \nabla A$ .

*Proof.* See Appendix A, Lemma A.2.  $\square$

Let  $A = A_\theta$  in Lemma 2 (i), we have

$$\nabla_\theta \log \pi = \frac{1}{\tau} (\mathbf{I} - \pi) \nabla_\theta A_\theta.$$

Notice that  $\nabla_\theta f_1(A_\theta)$  is the gradient ascent direction of the policy evaluation and  $\nabla_\theta \log \pi$  is the gradient ascent direction of the policy improvement. Since  $\pi$  is a constant when doing the policy evaluation, when solving for  $\nabla_\theta f_1(A_\theta) \propto \nabla_\theta \log \pi$ , we regard  $\pi$  as a constant and integrate  $(\mathbf{I} - \pi) \nabla_\theta A_\theta$ , then

$$f_1(A_\theta) \propto (\mathbf{I} - \pi) A_\theta + \text{constant}.$$

Again, since  $\mathbb{E}_\pi[Q] = V_\theta \Rightarrow \mathbb{E}_\pi[f_1(A_\theta)] = 0$ , we know

$$Q = (\mathbf{I} - \pi) A_\theta + V_\theta = A_\theta - \mathbb{E}_\pi[A_\theta] + V_\theta.$$

Reformatting the above derivation, we have the forward process of CASA. Denote  $\tau \in \mathbb{R}_+$  to be a positive temperature,  $sg$  to be stop gradient. CASA estimates  $V_\theta$ ,  $A_\theta$  by any function parameterized by  $\theta$  and calculates  $\pi_\theta$  and  $Q_\theta$  by

$$\begin{cases} \pi_\theta = \text{softmax}(A_\theta/\tau), \\ \bar{A}_\theta = A_\theta - \mathbb{E}_\pi[A_\theta],^2 & Q_\theta = \bar{A}_\theta + sg(V_\theta). \end{cases} \quad (1)$$

Note that there exist two  $sg$  operators in (1). The first  $sg$  operator exists in  $\bar{A}_\theta = A_\theta - \mathbb{E}_\pi[A_\theta] = A_\theta - sg(\pi_\theta) \cdot A_\theta$ . This  $sg$  operator guarantees the path consistency between the policy improvement and the policy evaluation, shown later in (8). Intuitively, this  $sg$  operator means that we keep  $\pi_\theta$  as a constant during the policy evaluation. The second  $sg$  operator exists in  $Q_\theta = \bar{A}_\theta + sg(V_\theta)$ . This  $sg$  operator is crucial in the convergence proof of Theorem 3. As (Chen & He, 2020) regards  $sg$  in siamese representation learning as a case of EM-algorithm (Dempster et al., 1977), a similar interpretation exists here.  $Q_\theta = \bar{A}_\theta + sg(V_\theta)$  decomposes the estimation of  $Q_\theta$  into a two stage problem, where the first is to estimate the advantage of each action without changing the expectation, the second is to estimate the expectation of  $Q_\theta$ .

Moreover, (1) is also a refinement of the structure of dueling- $Q$  learning (Wang et al., 2016). We know dueling- $Q$  estimates  $Q$  by  $Q = A + V$ , which is identical to the following Bellman equation

$$\mathcal{T}Q^\pi(s_t, a_t) = \mathbb{E}_p[r_t + \gamma V^\pi(s_{t+1}) - V^\pi(s_t)] + V^\pi(s_t).$$

<sup>2</sup> $\mathbb{E}_\pi[A_\theta] = sg(\pi) \cdot A_\theta$ , where  $\cdot$  represents inner product.

Since  $\mathbb{E}_\pi[\mathbb{E}_p[r_t + \gamma V^\pi(s_{t+1}) - V^\pi(s_t)]] = 0$ , we have

$$\begin{aligned} \mathcal{T}Q^\pi(s_t, a_t) &= \mathbb{E}_p[r_t + \gamma V^\pi(s_{t+1}) - V^\pi(s_t)] \\ &\quad - \mathbb{E}_\pi[\mathbb{E}_p[r_t + \gamma V^\pi(s_{t+1}) - V^\pi(s_t)] + V^\pi(s_t)], \end{aligned}$$

which is  $Q = A - \mathbb{E}_\pi[A] + V$ . This is exactly how we estimates  $Q$  in (1). This formulation introduces the necessary condition  $\mathbb{E}_\pi[Q] = V$ , without loss of generality.

We provide a summary of the above structure as shown in Figure 3.

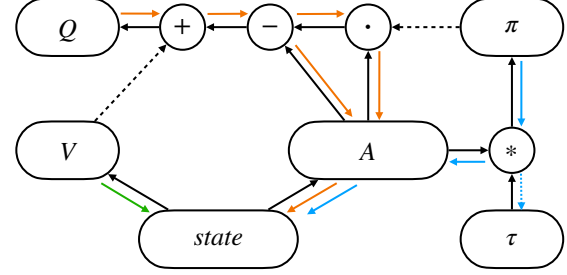


Figure 3. **Black** lines represent the forward process. **Dotted black** lines represent the *stop gradient* operator in the forward process. **Colorful** lines represent backpropagation from different loss functions. Specifically, **blue** lines represent  $\mathbb{E}_\pi[(G - V) \nabla \log \pi]$ , **orange** lines represent  $\mathbb{E}_\pi[(G - Q) \nabla Q]$ , and **green** lines represent  $\mathbb{E}_\pi[(G - V) \nabla V]$ .

### 3.3. DR-Trace and Off-Policy Training

For brevity, we omit  $\theta$  and  $V, Q, A, \pi$  are all approximated functions.

One simple choice is to learn  $V$  and  $\pi$  by V-Trace (Espeholt et al., 2018) and to learn  $Q$  by ReTrace (Munos et al., 2016). (Espeholt et al., 2018) shows that  $V^{\tilde{\pi}}$  estimated by V-Trace converges to  $V^*$  that corresponds to some  $\tilde{\pi}_{VTrace}$ . Respectively, (Munos et al., 2016) shows that  $Q^{\tilde{\pi}}$  estimated by ReTrace converges to  $Q^*$  that corresponds to some  $\tilde{\pi}_{ReTrace}$ .

Though we can apply V-Trace to learn  $(V, \pi)$  and ReTrace to learn  $Q$ , it's inadequate. As CASA estimates  $(V, Q, \pi)$ , two questions come accordingly, **i)** how to guarantee that  $\tilde{\pi}_{VTrace} = \tilde{\pi}_{ReTrace}$ , **ii)** how to exploit  $(V, Q, \pi)$  to make a better estimation. Inspired by Doubly Robust (Jiang & Li, 2016), which is shown to maximally reduce the variance, we introduce DR-Trace, which estimates  $V$  by

$$V_{DR}^{\tilde{\pi}}(s_t) \stackrel{def}{=} \mathbb{E}_{\mu, p}[V(s_t) + \sum_{k \geq 0} \gamma^k c_{[t:t+k-1]} \rho_{t+k} \delta_{t+k}^{DR} V], \quad (2)$$

where  $\delta_t^{DR} V \stackrel{def}{=} r_t + \gamma V(s_{t+1}) - Q(s_t, a_t)$  is one-step Doubly Robust error,  $\rho_t \stackrel{def}{=} \min\{\frac{\pi_t}{\mu_t}, \bar{\rho}\}$  and  $c_t \stackrel{def}{=} \min\{\frac{\pi_t}{\mu_t}, \bar{c}\}$



are clipped per-step importance sampling,  $c_{[t:t+k]} \stackrel{\text{def}}{=} \prod_{i=0}^k c_{t+i}$ .

With one step Bellman equation, we estimate  $Q$  by

$$\begin{aligned} Q_{DR}^{\tilde{\pi}}(s_t, a_t) &\stackrel{\text{def}}{=} \mathbb{E}_{s_{t+1}, r_t \sim p(\cdot, \cdot | s_t, a_t)} [r_t + \gamma V_{DR}^{\tilde{\pi}}(s_{t+1})] \\ &= \mathbb{E}_{\mu, p} [Q(s_t, a_t) + \sum_{k \geq 0} \gamma^k c_{[t+1:t+k-1]} \tilde{\rho}_{t,k} \delta_{t+k}^{DR} V], \end{aligned} \quad (3)$$

where  $\tilde{\rho}_{t,k} = 1_{\{k=0\}} + 1_{\{k>0\}} \rho_{t+k}$ .

**Theorem 3.** Define  $\bar{A} = A - \mathbb{E}_{\pi}[A]$ ,  $Q = \bar{A} + sg(V)$ ,

$$\mathcal{T}(Q) \stackrel{\text{def}}{=} \mathbb{E}_{\mu, p} [Q(s_t, a_t) + \sum_{k \geq 0} \gamma^k c_{[t+1:t+k-1]} \tilde{\rho}_{t,k} \delta_{t+k}^{DR} V],$$

$$\mathcal{S}(V) \stackrel{\text{def}}{=} \mathbb{E}_{\mu, p} [V(s_t) + \sum_{k \geq 0} \gamma^k c_{[t:t+k-1]} \rho_{t,k} \delta_{t+k}^{DR} V],$$

$$\mathcal{U}(Q, V) = (\mathcal{T}(Q) - \mathbb{E}_{\pi}[Q] + \mathcal{S}(V), \mathcal{S}(V)),$$

$$\mathcal{U}^{(n)}(Q, V) = \mathcal{U}(\mathcal{U}^{(n-1)}(Q, V)),$$

then  $\mathcal{U}^{(n)}(Q, V) \rightarrow (Q^{\tilde{\pi}}, V^{\tilde{\pi}})$  that corresponds to

$$\tilde{\pi}(a|s) = \frac{\min \{\bar{\rho}\mu(a|s), \pi(a|s)\}}{\sum_{b \in \mathcal{A}} \min \{\bar{\rho}\mu(b|s), \pi(b|s)\}}.$$

as  $n \rightarrow +\infty$ .

*Proof.* See Appendix A, Theorem A.1.  $\square$

Theorem 3 shows that DR-Trace is a contraction mapping and  $(V, Q)$  converges to  $(V^{\tilde{\pi}}, Q^{\tilde{\pi}})$  that corresponds to

$$\tilde{\pi}(a|s) = \frac{\min \{\bar{\rho}\mu(a|s), \pi(a|s)\}}{\sum_{b \in \mathcal{A}} \min \{\bar{\rho}\mu(b|s), \pi(b|s)\}}. \quad (4)$$

At training time, the policy evaluation is achieved by updating  $\theta$  to minimize  $l_2$  losses

$$\begin{aligned} \mathcal{V}(\theta) &= \mathbb{E}_{\pi} [(V_{\theta}(s_t) - V_{DR}^{\tilde{\pi}}(s_t))^2], \\ \mathcal{Q}(\theta) &= \mathbb{E}_{\pi} [(Q_{\theta}(s_t, a_t) - Q_{DR}^{\tilde{\pi}}(s_t, a_t))^2], \end{aligned}$$

which gives the ascent direction of  $\theta$  by

$$\begin{aligned} \nabla_{\theta} \mathcal{V}(\theta) &= \mathbb{E}_{\pi} [(V_{DR}^{\tilde{\pi}}(s_t) - V_{\theta}(s_t)) \nabla V_{\theta}(s_t)], \\ \nabla_{\theta} \mathcal{Q}(\theta) &= \mathbb{E}_{\pi} [(Q_{DR}^{\tilde{\pi}}(s_t, a_t) - Q_{\theta}(s_t, a_t)) \nabla Q_{\theta}(s_t, a_t)]. \end{aligned} \quad (5)$$

And we make the policy improvement by policy gradient, which gives the ascent direction of  $\theta$  by

$$\nabla_{\theta} \mathcal{J}(\tau, \theta) = \mathbb{E}_{\mu} [\tau \rho_t (Q_{DR}^{\tilde{\pi}}(s_t, a_t) - V_{\theta}(s_t)) \nabla_{\theta} \log \pi_t], \quad (6)$$

where  $\mathcal{J}(\tau, \theta) = \tau \mathbb{E}_{\pi} [\sum \gamma^t r_t]$ . It takes an additional  $\tau$ , which frees the scale of gradient from  $\tau$ .

Finally, the gradient ascent direction of  $\theta$  is given by

$$\alpha_1 \nabla_{\theta} \mathcal{V} + \alpha_2 \nabla_{\theta} \mathcal{Q} + \alpha_3 \nabla_{\theta} \mathcal{J}. \quad (7)$$

### 3.4. Path Consistency Between Policy Evaluation and Policy Improvement

Now we discuss how the policy evaluation and the policy improvement affect each other.

With  $(V, Q, \pi)$  defined in (1), by Lemma 2, we have

$$\nabla_{\theta} Q = (\mathbf{1} - \pi) \nabla_{\theta} A = \tau \nabla_{\theta} \log \pi. \quad (8)$$

For brevity, denote  $\mathbf{g} = (\mathbf{1} - \pi) \nabla_{\theta} A$ .

Plugging (8) into (5) (6), we have

$$\nabla_{\theta} \mathcal{Q} = \mathbb{E}_{\pi} [(Q_t^{\tilde{\pi}} - Q_t) \mathbf{g}], \quad \nabla_{\theta} \mathcal{J} = \mathbb{E}_{\pi} [(Q_t^{\tilde{\pi}} - V_t) \mathbf{g}].^3 \quad (9)$$

Recalling Theorem 3, when the importance sampling ratio  $\bar{\rho} = +\infty$  and we ignore the bias introduced by the function approximation error, we know  $Q_t^{\tilde{\pi}}$  is an unbiased estimation of  $\mathbb{E}_{\pi}[G_t | s_t, a_t]$ . Based on this observation,  $\nabla_{\theta} \mathcal{Q}$  is a typical policy evaluation that  $Q$  converges to  $\mathbb{E}_{\pi}[\sum \gamma^k r_k | s, a]$ , and  $\nabla_{\theta} \mathcal{J}$  is a typical policy improvement that maximizes  $\mathbb{E}_{\pi}[\sum \gamma^k r_k]$ .

For equation (9), there is another thing in common, which is  $\mathbf{g}$ , the direction of the gradient. We call it a path. (9) shows that  $\nabla_{\theta} \mathcal{Q}$  and  $\nabla_{\theta} \mathcal{J}$  walk along the same path  $\mathbf{g}$ . The only difference is that  $\nabla_{\theta} \mathcal{Q}$  walks with step size  $Q_t^{\tilde{\pi}} - Q_t$ , but  $\nabla_{\theta} \mathcal{J}$  walks with step size  $Q_t^{\tilde{\pi}} - V_t$ . When we share all variables to estimate  $Q$  and  $\pi$ , except for  $\tau$ , this is exactly the case  $\beta = 0$  in Figure 1. Under such condition, there is no gradient conflict between the policy improvement and the policy evaluation. This is why we call the algorithm Critic AS an Actor.

If we make a subtraction between  $\nabla_{\theta} \mathcal{Q}$  and  $\nabla_{\theta} \mathcal{J}$ , we have

$$\nabla_{\theta} \mathcal{Q} = \nabla_{\theta} \mathcal{J} - \mathbb{E}_{\pi} [(Q_t - V_t) \mathbf{g}]. \quad (10)$$

We know  $\mathbb{E}_{\pi} [(Q_t - V_t) \mathbf{g}]$  is also a policy gradient with function approximated  $Q_t$ . If we regard  $Q_t^{\tilde{\pi}}$  as a *better* estimation of  $Q_t$ , (10) says that the policy evaluation equals to the policy improvement minus a *worse* policy improvement, which is to retain the policy evaluation by pulling back from the policy improvement. As for how *worse* it is, it depends on how far  $Q_t$  is from  $Q_t^{\tilde{\pi}}$ . Recalling (9) and  $\mathbf{g} = \tau \nabla_{\theta} \log \pi$ , we observe that if  $Q_t$  underestimates  $Q_t^{\tilde{\pi}}$ ,  $\nabla_{\theta} \mathcal{Q}$  promotes  $\pi(a_t | s_t)$  by  $Q_t^{\tilde{\pi}} - Q_t$ , otherwise  $\nabla_{\theta} \mathcal{Q}$  diminishes  $\pi(a_t | s_t)$  by  $Q_t^{\tilde{\pi}} - Q_t$ . So except for the policy evaluation,  $\nabla_{\theta} \mathcal{Q}$  does do policy improvement along the same path as  $\nabla_{\theta} \mathcal{J}$ , but only to compensate the estimation error of  $Q_t$ .

**Lemma 4.** Define  $\bar{A} = A - \mathbb{E}_{\pi}[A]$ ,  $Q = \bar{A} + sg(V)$ ,  $\pi = \text{softmax}(A/\tau)$ , then  $\mathbb{E}_{\pi} [(Q - V) \nabla \log \pi] = -\tau \nabla \mathbf{H}[\pi]$ .

*Proof.* See Appendix A, Lemma A.3.  $\square$

<sup>3</sup> $Q_t^{\tilde{\pi}} = Q_{DR}^{\tilde{\pi}}(s_t, a_t)$ ,  $Q_t = Q(s_t, a_t)$ ,  $V_t = V(s_t)$ .

Table 1. Atari Scores. Rainbow’s scores are from (Hessel et al., 2017). IMPALA’s scores are from (Espeholt et al., 2018). LASER’s scores are from (Schmitt et al., 2020), no sweep at 200M.

	Mean HNS	Median HNS	Mean SABER	Median SABER
Rainbow	873.97	230.99	28.39	4.92
IMPALA	957.34	191.82	29.45	4.31
LASER	1741.36	<b>454.91</b>	<b>36.77</b>	8.08
<b>CASA</b>	<b>1929.95</b>	195.54	35.91	<b>8.73</b>

Now we know  $\nabla_{\theta} Q$  is not only a policy evaluation but is also equivalent to a compensational policy improvement. If we further exploit the structural information, by Lemma 4,

$$\mathbb{E}_{\pi} [(Q_t - V_t)\mathbf{g}] = \tau \mathbb{E}_{\pi} [(Q_t - V_t)\nabla_{\theta} \log \pi] = -\tau^2 \nabla_{\theta} \mathbf{H}[\pi],$$

we have

$$\nabla_{\theta} Q = \nabla_{\theta} \mathcal{J} + \tau^2 \nabla_{\theta} \mathbf{H}[\pi]. \quad (11)$$

(11) shows another explanation of  $\nabla_{\theta} Q$ , which is a policy gradient with entropy regularization. As long as  $\alpha_2 > 0$  in (7), an entropy regularization is introduced by  $\alpha_2 \nabla_{\theta} Q$ . An intuitive explanation is that, as  $Q$  and  $\pi$  share  $A$ , but the target of  $Q$  is dominated by MDP, so  $Q$  regularizes  $A$  to prevent  $\pi$  from collapse to trivial solutions.

## 4. Experiments

In this section, we firstly introduce our basic setup. Then we report our results on ALE, namely, 57 atari games. To further investigate how CASA works, we study the effects of  $sg$  operators, DR-Trace and path consistency.

### 4.1. Basic Setup

We use Learner-Actor architecture for large scale training. To deal with partially observable MDP (POMDP), we use a recurrent encoder by LSTM (Schmidhuber, 1997) with 256 units. We use *burn-in* (Kapturowski et al., 2018) to deal with representational drift. We store the recurrent state during inference and make it the start point of the *burn-in* phase. We train each sample twice. We use no intrinsic reward in any experiment. To be general, we will not end the episode if life is lost. All hyperparameters are listed in Appendix B.

### 4.2. Analysis and Summary of Results

Table 1 summarizes the mean and the median Human Normalized Scores (HNS) and Standardized Atari BENCHMARK for RL (SABER) (Toromanoff et al., 2019). Scores of 57 games and the corresponding learning curves are listed in Appendix C.

In general, CASA meets the comparable performance compared with other strong baselines. CASA also achieves the highest mean HNS and the highest median SABER among 200M scale experiments.

The results can roughly be classified into three kinds. (i) CASA achieves historical highest score on some games, such as Atlantis, Enduro, DemonAttack. (ii) The learning processes of some games have not converged, such as Alien, BeamRider, ChopperCommand. This suggest two potential improvements. One is that a larger training scale is expected to further boost the score. The other is to improve the methodology. Compared with LASER on Alien, Centipede, we find there is room for higher sample efficiency. (iii) CASA suffers from the hard exploration problem, such as IceHockey, PrivateEye, Surround. Previous studies (Burda et al., 2018; Badia et al., 2020b) have tried to overcome the challenges of exploration from different aspects. One possible way to mitigate the problem is combining CASA with these techniques. The other specific way for CASA is how to balance exploration and exploitation explicitly. Recalling (11), although CASA does not need any entropy regularization, it’s still a problem to choose a proper temperature  $\tau$ . The balance between exploration and exploitation induced by  $\tau$  is implicit rather than explicit. If we can control the balance by adjusting some parameter explicitly in a closed-form function of the target policy, we can find a better adaptive method for exploration.

### 4.3. Ablation Study

We check the following aspects of CASA. (i) *stop gradient* of  $\pi$  in  $\bar{A} = A - \mathbb{E}_{\pi}[A] = A - sg(\pi) \cdot A$ , which gives the path consistency. The ablation study removes  $sg$  operator, so the path consistency cannot hold. (ii) *stop gradient* of  $V$  in  $Q = \bar{A} + sg(V)$ , which is crucial in the convergence proof of Theorem 3. The ablation study removes  $sg$ , so the convergence property of DR-Trace cannot be guaranteed. (iii) DR-Trace, which is to reduce the variance of the policy evaluation maximally. The ablation study uses V-Trace to estimate state value and ReTrace to estimate state-action value instead of DR-Trace, which aims to check the efficiency of DR-Trace. (iv) The path consistency property between the policy evaluation and the policy improvement. Since the gradient directions of  $Q$ -loss and  $\pi$ -loss are identical, it should be less influenced by the scale of the step-size, which meets the motivation in Figure 1. The ablation study samples the coefficients of  $Q$ -loss and  $\pi$ -loss for every sample of every batch. If the path consistency property holds, it should perform similar to the original CASA. All ablation settings are listed in Table 2.

We do ablation study on three different games, Breakout, ChopperCommand and Krull. We choose Breakout because most algorithms can achieve a better result on it with a

Table 2. Ablation Settings. The baseline of these ablation changes is **original CASA**. Except for the changes listed in the table, there is no other change of CASA in each ablation case.

Name	Origin	Change(s)
CASA	N/A	N/A
<i>no_stop_π</i>	$\bar{A} = A - \mathbb{E}_\pi[A] = A - sg(\pi) \cdot A \Rightarrow$	$\bar{A} = A - \pi \cdot A$
<i>no_stop_v</i>	$Q = \bar{A} + sg(V) \Rightarrow$	$Q = \bar{A} + V$
<i>no_drtrace</i>	$V_\theta$ is estimated by DR-Trace $Q_\theta$ is estimated by DR-Trace $\Rightarrow$	$V_\theta$ is estimated by V-Trace $Q_\theta$ is estimated by ReTrace
<i>random_scaling</i>	$Q$ -loss Scaling $\alpha_2 = 10.0$ $\pi$ -loss Scaling $\alpha_3 = 10.0$ $\Rightarrow$	$\alpha_2 \sim Uniform([0.0, 20.0])$ $\alpha_3 \sim Uniform([0.0, 20.0])$

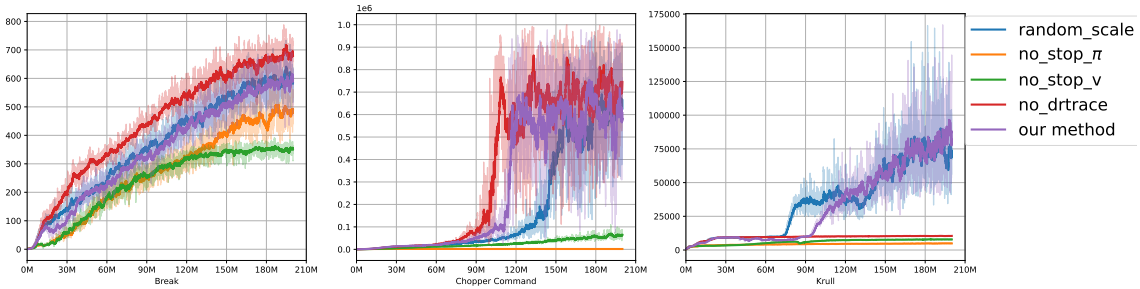


Figure 4. Evaluation Return Curves.

large training scale. But it’s not easy to get an extreme high score on it. So it’s a good benchmark to verify the sample efficiency. We choose ChopperCommand and Krull, because we find there exists a breakthrough moment for each game. Some algorithms can make a breakthrough, while some cannot. We do not choose any hard-to-explore games for ablation study, such as Pitfall, MontezumaRevenge. This is because CASA is not designed to solve these problems and have not approached the average human performance on these games. It’s not convincing to do ablation study when the baseline performs poor on these games.

Our ablation results are shown in Figure 4. It’s obvious that *no\_stop\_π* and *no\_stop\_v* perform the worst among others. They show a lower sample efficiency on Breakout and have not made a breakthrough on ChopperCommand and Krull. This phenomenon proves the two *sg* operators defined in the definition of CASA (1) are necessary. One is for the path consistency property and the other is for the convergence property of DR-Trace. As for *random\_scaling*, though it shows a lower sample efficiency on ChopperCommand and a higher sample efficiency on Krull, the overall performance is similar to CASA. When the path of the policy improvement and the policy evaluation is consistent, CASA can resist the noise from the scaling of  $Q$ -loss and  $\pi$ -loss. This ablation study proves that the path consistency property does exist and follows the motivation illustrated in Figure 1. For *no\_drtrace*, we find it performs better on Breakout, shows

a higher sample efficiency on ChopperCommand, but fails to make a breakthrough on Krull. Recalling the fact that Doubly Robust can maximally reduce the variance of the Bellman error, it seems that such phenomenon is explainable. Since *no\_drtrace* has a higher variance, it’s less stable but also potential to achieve a better performance. A conclusion cannot be made about *no\_drtrace*, as this phenomenon means that *no\_drtrace* is less stable than DR-Trace, but it also holds the potential to achieve a better performance.

## 5. Conclusion

This paper proposes a novel method which aims to resolve the inconsistency between the policy improvement and the policy evaluation steps in GPI. To this end, we propose an innovative actor-critic design termed **Critic AS** an Actor (CASA) which consolidates the policy improvement and policy evaluation with a more guaranteed policy improvement. We present both sophisticated theoretical proof as well as empirical evaluation for CASA. The results show that our proposed method could achieve state-of-the-art performance standard with noticeable performance gain over several strong baselines when evaluated on ALE 200 million (200M) test suite. We also present several ablation case study, which demonstrates the effectiveness of the proposed method’s theoretical properties. Future work includes studying alternative properties of GPI to improve consistency.

## References

- Badia, A. P., Piot, B., Kapturowski, S., Sprechmann, P., Vitvitskyi, A., Guo, D., and Blundell, C. Agent57: Outperforming the atari human benchmark. *arXiv preprint arXiv:2003.13350*, 2020a.
- Badia, A. P., Sprechmann, P., Vitvitskyi, A., Guo, D., Piot, B., Kapturowski, S., Tieleman, O., Arjovsky, M., Pritzel, A., Bolt, A., et al. Never give up: Learning directed exploration strategies. *arXiv preprint arXiv:2002.06038*, 2020b.
- Bellemare, M. G., Naddaf, Y., Veness, J., and Bowling, M. The arcade learning environment: An evaluation platform for general agents. *Journal of Artificial Intelligence Research*, 47:253–279, jun 2013.
- Burda, Y., Edwards, H., Storkey, A., and Klimov, O. Exploration by random network distillation. *arXiv preprint arXiv:1810.12894*, 2018.
- Chen, X. and He, K. Exploring simple siamese representation learning. *arXiv preprint arXiv:2011.10566*, 2020.
- Dempster, A. P., Laird, N. M., and Rubin, D. B. Maximum likelihood from incomplete data via the em algorithm. *JOURNAL OF THE ROYAL STATISTICAL SOCIETY, SERIES B*, 39(1):1–38, 1977.
- Espeholt, L., Soyer, H., Munos, R., Simonyan, K., Mnih, V., Ward, T., Doron, Y., Firoiu, V., Harley, T., Dunning, I., et al. Impala: Scalable distributed deep-rl with importance weighted actor-learner architectures. *arXiv preprint arXiv:1802.01561*, 2018.
- Ghosh, D., Machado, M. C., and Roux, N. L. An operator view of policy gradient methods. *ArXiv*, abs/2006.11266, 2020.
- Haarnoja, T., Zhou, A., Abbeel, P., and Levine, S. Soft actor-critic: Off-policy maximum entropy deep reinforcement learning with a stochastic actor. *arXiv preprint arXiv:1801.01290*, 2018.
- Hessel, M., Modayil, J., Van Hasselt, H., Schaul, T., Ostrovski, G., Dabney, W., Horgan, D., Piot, B., Azar, M., and Silver, D. Rainbow: Combining improvements in deep reinforcement learning. *arXiv preprint arXiv:1710.02298*, 2017.
- Jiang, N. and Li, L. Doubly robust off-policy value evaluation for reinforcement learning. In *International Conference on Machine Learning*, pp. 652–661. PMLR, 2016.
- Kapturowski, S., Ostrovski, G., Quan, J., Munos, R., and Dabney, W. Recurrent experience replay in distributed reinforcement learning. In *International conference on learning representations*, 2018.
- Machado, M. C., Bellemare, M. G., Talvitie, E., Veness, J., Hausknecht, M. J., and Bowling, M. Revisiting the arcade learning environment: Evaluation protocols and open problems for general agents. *Journal of Artificial Intelligence Research*, 61:523–562, 2018.
- Mnih, V., Kavukcuoglu, K., Silver, D., Rusu, A. A., Veness, J., Bellemare, M. G., Graves, A., Riedmiller, M., Fidjeland, A. K., Ostrovski, G., et al. Human-level control through deep reinforcement learning. *nature*, 518(7540): 519–523, 2015.
- Mnih, V., Badia, A. P., Mirza, M., Graves, A., Lillicrap, T. P., Harley, T., Silver, D., and Kavukcuoglu, K. Asynchronous methods for deep reinforcement learning, 2016.
- Munos, R., Stepleton, T., Harutyunyan, A., and Bellemare, M. Safe and efficient off-policy reinforcement learning. In Lee, D. D., Sugiyama, M., Luxburg, U. V., Guyon, I., and Garnett, R. (eds.), *Advances in Neural Information Processing Systems 29*, pp. 1054–1062. Curran Associates, Inc., 2016.
- Pedersen, C. L. Re: Human-level performance in 3d multiplayer games with population-based reinforcement learning. *Science*, 2019.
- Schaul, T., Quan, J., Antonoglou, I., and Silver, D. Prioritized experience replay. *arXiv preprint arXiv:1511.05952*, 2015.
- Schmidhuber, S. H. J. Long short-term memory. *Neural Computation*, 1997.
- Schmitt, S., Hessel, M., and Simonyan, K. Off-policy actor-critic with shared experience replay. In *International Conference on Machine Learning*, pp. 8545–8554. PMLR, 2020.
- Schulman, J., Levine, S., Abbeel, P., Jordan, M., and Moritz, P. Trust region policy optimization. In *International conference on machine learning*, pp. 1889–1897, 2015a.
- Schulman, J., Moritz, P., Levine, S., Jordan, M., and Abbeel, P. High-dimensional continuous control using generalized advantage estimation. *arXiv preprint arXiv:1506.02438*, 2015b.
- Schulman, J., Wolski, F., Dhariwal, P., Radford, A., and Klimov, O. Proximal policy optimization algorithms. *arXiv preprint arXiv:1707.06347*, 2017.
- Sutton, R. S. and Barto, A. G. *Reinforcement learning: An introduction*. MIT press, 2018.
- Toromanoff, M., Wirbel, E., and Moutarde, F. Is deep reinforcement learning really superhuman on atari? leveling the playing field. *arXiv preprint arXiv:1908.04683*, 2019.



Vinyals, O., Babuschkin, I., Czarnecki, W. M., Mathieu, M., Dudzik, A., Chung, J., Choi, D. H., Powell, R., Ewalds, T., Georgiev, P., et al. Grandmaster level in starcraft ii using multi-agent reinforcement learning. *Nature*, 575 (7782):350–354, 2019.

Wang, Z., Schaul, T., Hessel, M., Hasselt, H., Lanctot, M., and Freitas, N. Dueling network architectures for deep reinforcement learning. In *International conference on machine learning*, pp. 1995–2003, 2016.

## A. Proofs

**Lemma A.1.** Let  $g \in \mathbf{C}^1(\mathbb{R}^n) : \mathbb{R}^n \rightarrow \mathbb{R}^n$ ,  $f \in \mathbf{C}^1(\mathbb{R}^{n+k}) : \mathbb{R}^{n+k} \rightarrow \mathbb{R}^n$ .

If  $\nabla_x g(x) = \nabla_x f(x, y)$ , for  $\forall x \in \mathbb{R}^n, y \in \mathbb{R}^k$ , then  $\exists c \in \mathbf{C}^1(\mathbb{R}^k) : \mathbb{R}^k \rightarrow \mathbb{R}^n$ , s.t.  $f(x, y) = g(x) + c(y)$ .

*Proof.* Let  $\tilde{f}(x, y) = f(x, y) - g(x)$ .

Since  $\nabla_x g(x) = \nabla_x f(x, y)$ , we have

$$\nabla_x \tilde{f} = 0, \text{ for } \forall x \in \mathbb{R}^n, y \in \mathbb{R}^k.$$

So  $\tilde{f}$  is a constant function w.r.t  $x$ , which can be denoted as  $c(y) = \tilde{f}(x, y)$ .

Hence,  $f(x, y) = g(x) + c(y)$ . □

**Lemma A.2.** (i) Define  $\pi = \text{softmax}(A/\tau)$ , then  $\nabla \log \pi = (\mathbf{I} - \pi) \frac{\nabla A}{\tau}$ . (ii) Denote  $sg$  to be stop gradient and define  $\bar{A} = A - \mathbb{E}_\pi[A]$ ,  $Q = \bar{A} + sg(V)$ , then  $\nabla Q = (\mathbf{I} - \pi) \nabla A$ .

*Proof.* As  $Q = \bar{A} + sg(V) = A - sg(\pi) \cdot A + sg(V)$ , it's obvious that  $\nabla Q = (\mathbf{I} - \pi) \nabla A$ .

For  $\log \pi$ , it's a typical derivative of cross entropy, so we have  $\nabla \log \pi = (\mathbf{I} - \pi) \nabla (A/\tau) = (\mathbf{I} - \pi) \frac{\nabla A}{\tau}$ . □

**Lemma A.3.** Define  $\bar{A} = A - \mathbb{E}_\pi[A]$ ,  $Q = \bar{A} + sg(V)$ ,  $\pi = \text{softmax}(A/\tau)$ , then

$$\mathbb{E}_\pi [(Q - V) \nabla \log \pi] = -\tau \nabla \mathbf{H}[\pi].$$

*Proof.* Since

$$\pi = \exp(A/\tau)/Z, \quad Z = \int_{\mathcal{A}} \exp(A/\tau),$$

we have

$$A = \tau \log \pi + \tau \log Z.$$

Based on the observation that  $\mathbb{E}_\pi [f(s) \nabla \log \pi(\cdot|s)] = 0$ , we have

$$\mathbb{E}_\pi [\mathbb{E}_\pi[A] \cdot \nabla \log \pi] = 0,$$

$$\mathbb{E}_\pi [\log Z \cdot \nabla \log \pi] = 0.$$

On the one hand,

$$\begin{aligned} \mathbb{E}_\pi [(Q - V) \nabla \log \pi] &= \mathbb{E}_\pi [A \nabla \log \pi] - \mathbb{E}_\pi [\mathbb{E}_\pi[A] \cdot \nabla \log \pi] \\ &= \tau \mathbb{E}_\pi [\log \pi \nabla \log \pi] + \tau \mathbb{E}_\pi [\log Z \cdot \nabla \log \pi] \\ &= \tau \mathbb{E}_\pi [\log \pi \nabla \log \pi]. \end{aligned}$$

On the other hand,

$$\begin{aligned} \nabla \mathbf{H}[\pi] &= -\nabla \int_{\mathcal{A}} \pi_i \log \pi_i \\ &= -\int_{\mathcal{A}} \nabla \pi_i \cdot \log \pi_i - \int_{\mathcal{A}} \pi_i \nabla \log \pi_i \\ &= -\int_{\mathcal{A}} \pi_i \nabla \log \pi_i \cdot \log \pi_i - \int_{\mathcal{A}} \pi_i \frac{\nabla \pi_i}{\pi_i} \\ &= -\mathbb{E}_\pi [\log \pi \nabla \log \pi]. \end{aligned}$$

Hence,  $\mathbb{E}_\pi [(Q - V) \nabla \log \pi] = -\tau \nabla \mathbf{H}[\pi]$ . □

**Lemma A.4.** Define  $\bar{A} = A - \mathbb{E}_\pi[A]$ ,  $Q = \bar{A} + sg(V)$ , then operator

$$\mathcal{T}(Q) \stackrel{def}{=} \mathbb{E}_{\mu,p}[Q(s_t, a_t) + \sum_{k \geq 0} \gamma^k c_{[t+1:t+k-1]} \tilde{\rho}_{t,k} \delta_{t+k}^{DR} V]$$

is a contraction mapping w.r.t.  $Q$ .

**Remark.** Note that  $\mathcal{T}(Q)$  is exactly (3).

Since  $Q = A + sg(V)$ , the gradient of  $V$  is stopped when estimating  $Q$ , updating  $Q$  will not change  $V$ , which is equivalent to updating  $A$ . Without loss of generality, we assume  $V$  is fixed as  $V^*$  in the proof.

*Proof.*  $\bar{A} = A - \mathbb{E}_\pi[A]$  shows  $\mathbb{E}_\pi[\bar{A}] = 0$ , which guarantees that no matter how we update  $A$ , we always have  $\mathbb{E}_\pi[Q] = V^*$ .

Based on above observations, define

$$\widetilde{\mathcal{T}}(Q) \stackrel{def}{=} -\mathbb{E}_\pi[Q] + \mathcal{T}(Q).$$

It's obvious that we only need to prove  $\widetilde{\mathcal{T}}(Q)$  is a contraction mapping.

For brevity, we denote

$$Q_t = Q(s_t, a_t), A_t = A(s_t, a_t), V_t^* = V^*(s_t).$$

Notice that  $\tilde{\rho}_{t,0} = 1$ , similar to (Munos et al., 2016), we can rewrite  $\widetilde{\mathcal{T}}$  as

$$\begin{aligned} \widetilde{\mathcal{T}}(Q) &= \mathbb{E}_{\mu,p}[A_t + \sum_{k \geq 0} \gamma^k c_{[t+1:t+k-1]} \tilde{\rho}_{t,k} \delta_{t+k}^{DR} V] \\ &= \mathbb{E}_{\mu,p}[-V_t^* + \sum_{k \geq 0} \gamma^k c_{[t+1:t+k-1]} \tilde{\rho}_{t,k} r_{t+k} + \sum_{k \geq 0} \gamma^{k+1} c_{[t+1:t+k-1]} \Delta_k], \end{aligned} \quad (12)$$

where

$$\Delta_k = \mathbb{E}_{\mu,p}[\tilde{\rho}_{t,k} V_{t+k+1}^* - c_{t+k} \tilde{\rho}_{t,k+1} Q_{t+k+1} | \mathcal{F}_{t+k}].^4 \quad (13)$$

By definition of  $Q$ ,

$$\mathbb{E}_{\mu,p}[V_{t+k+1}^* | \mathcal{F}_{t+k}] = \mathbb{E}_{\mu,p}[\mathbb{E}_\pi[Q_{t+k+1} | \mathcal{F}_{t+k+1}] | \mathcal{F}_{t+k}],$$

we can rewrite (13) as

$$\Delta_k = \mathbb{E}_{\mu,p}[(\tilde{\rho}_{t,k} \frac{\pi_{t+k+1}}{\mu_{t+k+1}} - c_{t+k} \tilde{\rho}_{t,k+1}) Q_{t+k+1} | \mathcal{F}_{t+k}]. \quad (14)$$

For any  $Q^1 = A^1 + sg(V^*)$ ,  $Q^2 = A^2 + sg(V^*)$ , since

$$\mathbb{E}_{\mu,p}[(\tilde{\rho}_{t,k} \frac{\pi_{t+k+1}}{\mu_{t+k+1}} - c_{t+k} \tilde{\rho}_{t,k+1}) | \mathcal{F}_{t+k}] \geq 0,$$

by (12) (14), we have

$$\|\widetilde{\mathcal{T}}(Q^1) - \widetilde{\mathcal{T}}(Q^2)\| \leq \mathcal{C} \|Q^1 - Q^2\|,$$

where

$$\begin{aligned} \mathcal{C} &= \mathbb{E}_{\mu,p}[\sum_{k \geq 0} \gamma^{k+1} c_{[t+1:t+k-1]} (\tilde{\rho}_{t,k} \frac{\pi_{t+k+1}}{\mu_{t+k+1}} - c_{t+k} \tilde{\rho}_{t,k+1})] \\ &= \mathbb{E}_{\mu,p}[1 - 1 + \sum_{k \geq 0} \gamma^{k+1} c_{[t+1:t+k-1]} (\tilde{\rho}_{t,k} - c_{t+k} \tilde{\rho}_{t,k+1})] \\ &= 1 - (1 - \gamma) \mathbb{E}_{\mu,p}[\sum_{k \geq 0} \gamma^k c_{[t+1:t+k-1]} \tilde{\rho}_{t,k}] \\ &\leq 1 - (1 - \gamma) < 1. \end{aligned}$$

Hence,  $\widetilde{\mathcal{T}}(Q)$  is a contraction mapping and converges to some fixed function, which we denote as  $A^*$ . So  $\mathcal{T}(Q)$  is also a contraction mapping and converges to  $A^* + V^*$ .  $\square$

<sup>4</sup>  $\mathcal{F}$  represents filtration.

**Lemma A.5.** Define  $Q = A + sg(V)$  with  $\mathbb{E}_\pi[A] = 0$ , then operator

$$\mathcal{S}(V) \stackrel{\text{def}}{=} \mathbb{E}_{\mu,p}[V(s_t) + \sum_{k \geq 0} \gamma^k c_{[t:t+k-1]} \rho_{t,k} \delta_{t+k}^{DR} V]$$

is a contraction mapping w.r.t.  $V$ .

**Remark.** Note that  $\mathcal{S}(V)$  is exactly (2).

*Proof.* Same as Lemma A.4, we can get

$$\Delta_k = \mathbb{E}_{\mu,p} [(\rho_{t+k} - c_{t+k} \rho_{t+k+1}) V_{t+k+1} - c_{t+k} \rho_{t+k+1} A_{t+k+1}^* | \mathcal{F}_{t+k}],$$

so we have

$$\Delta_k^1 - \Delta_k^2 = \mathbb{E}_{\mu,p} [(\rho_{t+k} - c_{t+k} \rho_{t+k+1}) \cdot (V_{t+k+1}^1 - V_{t+k+1}^2) | \mathcal{F}_{t+k}].$$

The proof attributes to (Espeholt et al., 2018). □

**Theorem A.1.** Define  $\bar{A} = A - \mathbb{E}_\pi[A]$ ,  $Q = \bar{A} + sg(V)$ . Define

$$\begin{aligned} \mathcal{T}(Q) &\stackrel{\text{def}}{=} \mathbb{E}_{\mu,p}[Q(s_t, a_t) + \sum_{k \geq 0} \gamma^k c_{[t+1:t+k-1]} \tilde{\rho}_{t,k} \delta_{t+k}^{DR} V], \\ \mathcal{S}(V) &\stackrel{\text{def}}{=} \mathbb{E}_{\mu,p}[V(s_t) + \sum_{k \geq 0} \gamma^k c_{[t:t+k-1]} \rho_{t,k} \delta_{t+k}^{DR} V], \\ \mathcal{U}(Q, V) &= (\mathcal{T}(Q) - \mathbb{E}_\pi[Q] + \mathcal{S}(V), \mathcal{S}(V)), \\ \mathcal{U}^{(n)}(Q, V) &= \mathcal{U}(\mathcal{U}^{(n-1)}(Q, V)), \end{aligned}$$

then  $\mathcal{U}^{(n)}(Q, V) \rightarrow (Q^{\tilde{\pi}}, V^{\tilde{\pi}})$  that corresponds to

$$\tilde{\pi}(a|s) = \frac{\min \{\bar{\rho}\mu(a|s), \pi(a|s)\}}{\sum_{b \in \mathcal{A}} \min \{\bar{\rho}\mu(b|s), \pi(b|s)\}}.$$

as  $n \rightarrow +\infty$ .

**Remark.**  $\mathcal{T}(Q) - \mathbb{E}_\pi[Q] + \mathcal{S}(V)$  is **exactly** how  $Q$  is updated at training time. Since  $Q = A + sg(V)$ , if we apply gradient ascent on  $Q$  and  $V$  in directions (5) respectively, change of  $Q$  comes from two aspects. One comes from  $\nabla Q(\theta)$ , which changes  $A$ , the other comes from  $\nabla V(\theta)$ , which changes  $V$ . Because the gradient of  $V$  is stopped when estimating  $Q$ , the latter is captured by "minus old baseline, add new baseline", which is  $-\mathbb{E}_\pi[Q] + \mathcal{S}(V)$  in Theorem A.1.

*Proof.* Define

$$\begin{aligned} \widetilde{\mathcal{T}}(Q) &= -\mathbb{E}_\pi[Q] + \mathcal{T}(Q), \\ \widetilde{\mathcal{U}}(Q, V) &= (\widetilde{\mathcal{T}}(Q), \mathcal{S}(V)), \\ \widetilde{\mathcal{U}}^{(n)}(Q, V) &= \widetilde{\mathcal{U}}(\widetilde{\mathcal{U}}^{(n-1)}(Q, V)). \end{aligned}$$

By Lemma A.4,  $\widetilde{\mathcal{U}}^{(n)}(Q)$  converges to some  $A^*$  as  $n \rightarrow \infty$ . This process will not influence the estimation of  $V$  as the gradient of  $V$  is stopped when estimating  $Q$ . According to the proof,  $A^*$  does not depend on  $V$ .

By Lemma A.5,  $\mathcal{S}^{(n)}(V)$  converges to some  $V^*$  as  $n \rightarrow \infty$ .

Hence, we have

$$\widetilde{\mathcal{U}}^{(n)}(Q, V) \rightarrow (A^*, V^*) \text{ as } n \rightarrow +\infty.$$

By definition,

$$\mathcal{U}(Q, V) = (\widetilde{\mathcal{T}}(Q) + \mathcal{S}(V), \mathcal{S}(V)),$$

we can regard  $\widetilde{\mathcal{T}}(Q) + \mathcal{S}(V)$  as  $Q$  and regard  $\mathcal{S}(V)$  as  $V$ , then

$$\begin{aligned} \mathcal{U}^{(2)}(Q, V) &= \mathcal{U}(\widetilde{\mathcal{T}}(Q) + \mathcal{S}(V), \mathcal{S}(V)) \\ &= (\mathcal{T}(\widetilde{\mathcal{T}}(Q) + \mathcal{S}(V)) - \mathcal{S}(V) + \mathcal{S}^{(2)}(V), \mathcal{S}^{(2)}(V)) \\ &= (\widetilde{\mathcal{T}}^{(2)}(Q) + \mathcal{S}^{(2)}(V), \mathcal{S}^{(2)}(V)). \end{aligned}$$

By induction,

$$\begin{aligned}\mathcal{U}^{(n)}(Q, V) &= (\widetilde{\mathcal{T}}^{(n)}(Q) + \mathcal{J}^{(n)}(V), \mathcal{J}^{(n)}(V)) \\ &\rightarrow (A^* + V^*, V^*) \text{ as } n \rightarrow +\infty.\end{aligned}$$

Same as (Espeholt et al., 2018),

$$\tilde{\pi}(a|s) = \frac{\min\{\bar{\rho}\mu(a|s), \pi(a|s)\}}{\sum_{b \in \mathcal{A}} \min\{\bar{\rho}\mu(b|s), \pi(b|s)\}}.$$

is the policy s.t. the Bellman equation holds, which is

$$\mathbb{E}_{\mu}[\rho_t(r_t + \gamma V_{t+1} - V_t) | \mathcal{F}_t] = 0,$$

and  $\mathcal{U}(Q^{\tilde{\pi}}, V^{\tilde{\pi}}) = (Q^{\tilde{\pi}}, V^{\tilde{\pi}})$ .

So we have  $(A^* + V^*, V^*) = (Q^{\tilde{\pi}}, V^{\tilde{\pi}})$ . □



## B. Hyperparameters

Parameter	Value
Image Size	(84, 84)
Grayscale	Yes
Num. Action Repeats	4
Num. Frame Stacks	4
Action Space	Full
End of Episode When Life Lost	No
Num. States	200M
Sample Reuse	2
Num. Environments	160
Reward Shape	$\log(abs(r) + 1.0) \cdot (2 \cdot 1_{\{r \geq 0\}} - 1_{\{r < 0\}})$
Reward Clip	No
Random No-ops	30
Burn-in	40
Seq-length	80
Burn-in Stored Recurrent State	Yes
Bootstrap	Yes
Batch size	64
Discount ( $\gamma$ )	0.997
V-loss Scaling ( $\alpha_1$ )	1.0
Q-loss Scaling ( $\alpha_2$ )	10.0
$\pi$ -loss Scaling ( $\alpha_3$ )	10.0
Temperature ( $\tau$ )	1.0
DR-Trace Importance Sampling Clip $\bar{c}$	1.05
DR-Trace Importance Sampling Clip $\bar{\rho}$	1.05
Backbone	IMPALA,deep
LSTM Units	256
Optimizer	Adam Weight Decay
Weight Decay Rate	0.01
Weight Decay Schedule	Anneal linearly to 0
Learning Rate	5e-4
Warmup Steps	4000
Learning Rate Schedule	Anneal linearly to 0
AdamW $\beta_1$	0.9
AdamW $\beta_2$	0.98
AdamW $\epsilon$	1e-6
AdamW Clip Norm	50.0
Learner Push Model Every $n$ Steps	25
Actor Pull Model Every $n$ Steps	64

Table 3. Hyperparameters for Atari Experiments.

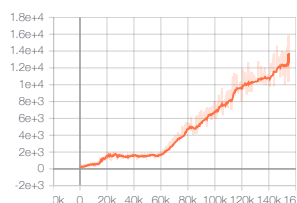
## C. Atari Results

Random scores and average human’s scores are from (Badia et al., 2020a). Human World Records (HWR) are from (Toromanoff et al., 2019). Rainbow’s scores are from (Hessel et al., 2017). IMPALA’s scores are from (Espeholt et al., 2018). LASER’s scores are from (Schmitt et al., 2020), no sweep at 200M.

Games	RND	HUMAN	RAINBOW	HNS(%)	IMPALA	HNS(%)	LASER	HNS(%)	CASA	HNS(%)
Scale			200M		200M		200M		200M	
alien	227.8	7127.8	9491.7	134.26	15962.1	228.03	<b>35565.9</b>	<b>512.15</b>	13720	195.54
amidar	5.8	1719.5	<b>5131.2</b>	<b>299.08</b>	1554.79	90.39	1829.2	106.4	560	32.34
assault	222.4	742	14198.5	2689.78	19148.47	3642.43	<b>21560.4</b>	<b>4106.62</b>	16228	3080.37
asterix	210	8503.3	<b>428200</b>	<b>5160.67</b>	300732	3623.67	240090	2892.46	213580	2572.80
asteroids	719	47388.7	2712.8	4.27	108590.05	231.14	<b>213025</b>	<b>454.91</b>	18621	38.36
atlantis	12850	29028.1	826660	5030.32	849967.5	5174.39	841200	5120.19	<b>3211600</b>	<b>19772.10</b>
bank heist	14.2	753.1	<b>1358</b>	<b>181.86</b>	1223.15	163.61	569.4	75.14	895.3	119.24
battle zone	236	37187.5	62010	167.18	20885	55.88	64953.3	175.14	<b>70137</b>	<b>189.17</b>
beam rider	363.9	16926.5	16850.2	99.54	32463.47	193.81	<b>90881.6</b>	<b>546.52</b>	34920	208.64
berzerk	123.7	2630.4	2545.6	96.62	1852.7	68.98	<b>25579.5</b>	<b>1015.51</b>	1648	60.81
bowling	23.1	160.7	30	5.01	59.92	26.76	48.3	18.31	<b>162.4</b>	<b>101.24</b>
boxing	0.1	12.1	99.6	829.17	99.96	832.17	<b>100</b>	<b>832.5</b>	98.3	818.33
breakout	1.7	30.5	417.5	1443.75	<b>787.34</b>	<b>2727.92</b>	747.9	2590.97	624.3	2161.81
centipede	2090.9	12017	8167.3	61.22	11049.75	90.26	<b>292792</b>	<b>2928.65</b>	102600	1012.57
chopper command	811	7387.8	16654	240.89	28255	417.29	<b>761699</b>	<b>11569.27</b>	616690	9364.42
crazy climber	10780.5	36829.4	<b>168788.5</b>	<b>630.80</b>	136950	503.69	167820	626.93	161250	600.70
defender	2874.5	18688.9	55105	330.27	185203	1152.93	336953	2112.50	<b>421600</b>	<b>2647.75</b>
demon attack	152.1	1971	111185	6104.40	132826.98	7294.24	133530	7332.89	<b>291590</b>	<b>16022.76</b>
double dunk	-18.6	-16.4	-0.3	831.82	-0.33	830.45	14	1481.82	<b>20.25</b>	<b>1765.91</b>
enduro	0	860.5	2125.9	247.05	0	0.00	0	0.00	<b>10019</b>	<b>1164.32</b>
fishing derby	-91.7	-38.8	31.3	232.51	44.85	258.13	45.2	258.79	<b>53.24</b>	<b>273.99</b>
freeway	0	29.6	<b>34</b>	<b>114.86</b>	0	0.00	0	0.00	3.46	11.69
frostbite	65.2	4334.7	<b>9590.5</b>	<b>223.10</b>	317.75	5.92	5083.5	117.54	1583	35.55
gopher	257.6	2412.5	70354.6	3252.91	66782.3	3087.14	114820.7	5316.40	<b>188680</b>	<b>8743.90</b>
gravitar	173	3351.4	1419.3	39.21	359.5	5.87	1106.2	29.36	<b>4311</b>	<b>130.19</b>
hero	1027	30826.4	<b>55887.4</b>	<b>184.10</b>	33730.55	109.75	31628.7	102.69	24236	77.88
ice hockey	-11.2	0.9	1.1	101.65	3.48	121.32	<b>17.4</b>	<b>236.36</b>	1.56	105.45
jamesbond	29	302.8	19809	72.24	601.5	209.09	<b>37999.8</b>	<b>13868.08</b>	12468	4543.10
kangaroo	52	3035	<b>14637.5</b>	<b>488.05</b>	1632	52.97	14308	477.91	5399	179.25
krull	1598	2665.5	8741.5	669.18	8147.4	613.53	9387.5	729.70	<b>64347</b>	<b>5878.13</b>
kung fu master	258.5	22736.3	52181	230.99	43375.5	191.82	<b>607443</b>	<b>2701.26</b>	124630.1	553.31
montezuma revenge	0	<b>4753.3</b>	384	8.08	0	0.00	0.3	0.01	2488.4	52.35
ms pacman	307.3	6951.6	5380.4	76.35	7342.32	105.88	6565.5	94.19	<b>7579</b>	<b>109.44</b>
name this game	2292.3	8049	13136	188.37	21537.2	334.30	26219.5	415.64	<b>32098</b>	<b>517.76</b>
phoenix	761.5	7242.6	108529	1662.80	210996.45	3243.82	<b>519304</b>	<b>8000.84</b>	498590	7681.23
pitfall	-229.4	<b>6463.7</b>	0	3.43	-1.66	3.40	-0.6	3.42	-17.8	3.16
pong	-20.7	14.6	20.9	117.85	20.98	118.07	<b>21</b>	<b>118.13</b>	20.39	116.40
private eye	24.9	<b>69571.3</b>	4234	6.05	98.5	0.11	96.3	0.10	134.1	0.16
qbert	163.9	13455.0	33817.5	253.20	<b>351200.12</b>	<b>2641.14</b>	21449.6	160.15	21043	157.09
riverraid	1338.5	17118.0	22920.8	136.77	29608.05	179.15	<b>40362.7</b>	<b>247.31</b>	11182	62.38
road runner	11.5	7845	62041	791.85	57121	729.04	45289	578.00	<b>251360</b>	<b>3208.64</b>
robotank	2.2	11.9	61.4	610.31	12.96	110.93	<b>62.1</b>	<b>617.53</b>	10.44	84.95
seaquest	68.4	<b>42054.7</b>	15898.9	37.70	1753.2	4.01	2890.3	6.72	11862	28.09
skiing	-17098	<b>-4336.9</b>	-12957.8	32.44	-10180.38	54.21	-29968.4	-100.86	-12730	34.23
solaris	1236.3	<b>12326.7</b>	3560.3	20.96	2365	10.18	2273.5	9.35	2319	9.76
space invaders	148	1668.7	18789	1225.82	43595.78	2857.09	<b>51037.4</b>	<b>3346.45</b>	3031	189.58
star gunner	664	10250	127029	1318.22	200625	2085.97	321528	3347.21	<b>337150</b>	<b>3510.18</b>
surround	-10	6.5	<b>9.7</b>	<b>119.39</b>	7.56	106.42	8.4	111.52	-10	0.00
tennis	-23.8	-8.3	0	153.55	0.55	157.10	<b>12.2</b>	<b>232.26</b>	-21.05	17.74
time pilot	3568	5229.2	12926	563.36	48481.5	2703.84	<b>105316</b>	<b>6125.34</b>	84341	4862.62
tutankham	11.4	167.6	241	146.99	292.11	179.71	278.9	171.25	<b>381</b>	<b>236.62</b>
up n down	533.4	11693.2	125755	1122.08	332546.75	2975.08	345727	3093.19	<b>416020</b>	<b>3723.06</b>
venture	0	<b>1187.5</b>	5.5	0.46	0	0.00	0	0.00	0	0.00
video pinball	0	17667.9	533936.5	3022.07	<b>572898.27</b>	<b>3242.59</b>	511835	2896.98	297920	1686.22
wizard of wor	563.5	4756.5	17862.5	412.57	9157.5	204.96	<b>29059.3</b>	<b>679.60</b>	26008	606.83
yars revenge	3092.9	54576.9	102557	193.19	84231.14	157.60	<b>166292.3</b>	<b>316.99</b>	76903.5	143.37
zaxxon	32.5	9173.3	22209.5	242.62	32935.5	359.96	41118	449.47	<b>46070.8</b>	<b>503.66</b>
MEAN HNS(%)	0.00	100.00		873.97		957.34		1741.36		<b>1929.95</b>
MEDIAN HNS(%)	0.00	100.00		230.99		191.82		<b>454.91</b>		195.54

# CASA: Bridging the Gap between Policy Improvement and Policy Evaluation with Conflict Averse Policy Iteration

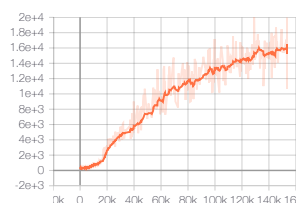
Games	RND	HWR	RAINBOW	SABER(%)	IMPALA	SABER(%)	LASER	SABER(%)	CASA	SABER(%)
Scale			200M		200M		200M		200M	
alien	227.8	<b>251916</b>	9491.7	3.68	15962.1	6.25	976.51	14.04	13720	5.36
amidar	5.8	<b>104159</b>	5131.2	4.92	1554.79	1.49	1829.2	1.75	560	0.53
assault	222.4	8647	14198.5	165.90	19148.47	200.00	<b>21560.4</b>	<b>200.00</b>	16228	189.99
asterix	210	<b>1000000</b>	428200	42.81	300732	30.06	240090	23.99	213580	21.34
asteroids	719	<b>10506650</b>	2712.8	0.02	108590.05	1.03	213025	2.02	18621	0.17
atlantis	12850	<b>10604840</b>	826660	7.68	849967.5	7.90	841200	7.82	3211600	30.20
bank heist	14.2	<b>82058</b>	1358	1.64	1223.15	1.47	569.4	0.68	895.3	1.07
battle zone	236	<b>801000</b>	62010	7.71	20885	2.58	64953.3	8.08	70137	8.73
beam rider	363.9	<b>999999</b>	16850.2	1.65	32463.47	3.21	90881.6	9.06	34920	3.46
berzerk	123.7	<b>1057940</b>	2545.6	0.23	1852.7	0.16	25579.5	2.41	1648	0.14
bowling	23.1	<b>300</b>	30	2.49	59.92	13.30	48.3	9.10	162.4	50.31
boxing	0.1	<b>100</b>	99.6	99.60	99.96	99.96	<b>100</b>	<b>100.00</b>	98.3	98.3
breakout	1.7	<b>864</b>	417.5	48.22	787.34	91.11	747.9	86.54	624.3	72.20
centipede	2090.9	<b>1301709</b>	8167.3	0.47	11049.75	0.69	292792	22.37	102600	7.73
chopper command	811	<b>999999</b>	16654	1.59	28255	2.75	761699	76.15	616690	61.64
crazy climber	10780.5	<b>219900</b>	168788.5	75.56	136950	60.33	167820	75.10	161250	71.95
defender	2874.5	<b>6010500</b>	55105	0.87	185203	3.03	336953	5.56	421600	6.97
demon attack	152.1	<b>1556345</b>	111185	7.13	132826.98	8.53	133530	8.57	291590	18.73
double dunk	-18.6	<b>21</b>	-0.3	46.21	-0.33	46.14	14	82.32	20.25	98.11
enduro	0	9500	2125.9	22.38	0	0.00	0	0.00	<b>10019</b>	<b>105.46</b>
fishing derby	-91.7	<b>71</b>	31.3	75.60	44.85	83.93	45.2	84.14	53.24	89.08
freeway	0	<b>38</b>	34	89.47	0	0.00	0	0.00	3.46	9.11
frostbite	65.2	<b>454830</b>	9590.5	2.09	317.75	0.06	5083.5	1.10	1583	0.33
gopher	257.6	<b>355040</b>	70354.6	19.76	66782.3	18.75	114820.7	32.29	188680	53.11
gravitar	173	<b>162850</b>	1419.3	0.77	359.5	0.11	1106.2	0.57	4311	2.54
hero	1027	<b>1000000</b>	55887.4	5.49	33730.55	3.27	31628.7	3.06	24236	2.32
ice hockey	-11.2	<b>36</b>	1.1	26.06	3.48	31.10	17.4	60.59	1.56	27.03
jamesbond	29	<b>45550</b>	19809	43.45	601.5	1.26	37999.8	83.41	12468	27.33
kangaroo	52	<b>1424600</b>	14637.5	1.02	1632	0.11	14308	1.00	5399	0.38
krull	1598	<b>104100</b>	8741.5	6.97	8147.4	6.39	9387.5	7.60	64347	61.22
kung fu master	258.5	<b>1000000</b>	52181	5.19	43375.5	4.31	607443	60.73	124630.1	12.44
montezuma revenge	0	<b>1219200</b>	384	0.03	0	0.00	0.3	0.00	2488.4	0.20
ms pacman	307.3	<b>290090</b>	5380.4	1.75	7342.32	2.43	6565.5	2.16	7579	2.51
name this game	2292.3	25220	13136	47.30	21537.2	83.94	26219.5	104.36	<b>32098</b>	<b>130.00</b>
phoenix	761.5	<b>4014440</b>	108529	2.69	210996.45	5.24	519304	12.92	498590	12.40
pitfall	-229.4	<b>114000</b>	0	0.20	-1.66	0.20	-0.6	0.20	-17.8	0.19
pong	-20.7	<b>21</b>	20.9	99.76	20.98	99.95	<b>21</b>	<b>100.00</b>	20.39	98.54
private eye	24.9	<b>101800</b>	4234	4.14	98.5	0.07	96.3	0.07	134.1	0.11
qbert	163.9	<b>2400000</b>	33817.5	1.40	351200.12	14.63	21449.6	0.89	21043	0.87
riverraid	1338.5	<b>1000000</b>	22920.8	2.16	29608.05	2.83	40362.7	3.91	11182	0.99
road runner	11.5	<b>2038100</b>	62041	3.04	57121	2.80	45289	2.22	251360	12.33
robotank	2.2	<b>76</b>	61.4	80.22	12.96	14.58	62.1	81.17	10.44	11.17
sequest	68.4	<b>999999</b>	15898.9	1.58	1753.2	0.17	2890.3	0.28	11862	1.18
skiing	-17098	<b>-3272</b>	-12957.8	29.95	-10180.38	50.03	-29968.4	-93.09	-12730	31.59
solaris	1236.3	<b>111420</b>	3560.3	2.11	2365	1.02	2273.5	0.94	2319	0.98
space invaders	148	<b>621535</b>	18789	3.00	43595.78	6.99	51037.4	8.19	3031	0.46
star gunner	664	77400	127029	164.67	200625	200.00	321528	200.00	<b>337150</b>	<b>200.00</b>
surround	-10	9.6	<b>9.7</b>	<b>100.51</b>	7.56	89.59	8.4	93.88	-10	0.00
tennis	-23.8	<b>21</b>	0	53.13	0.55	54.35	12.2	80.36	-21.05	6.14
time pilot	3568	65300	12926	15.16	48481.5	72.76	<b>105316</b>	<b>164.82</b>	84341	130.84
tutankham	11.4	<b>5384</b>	241	4.27	292.11	5.22	278.9	4.98	381	6.88
up n down	533.4	82840	125755	152.14	332546.75	200.00	345727	200.00	<b>416020</b>	<b>200.00</b>
venture	0	<b>38900</b>	5.5	0.01	0	0.00	0	0.00	0	0.00
video pinball	0	<b>89218328</b>	533936.5	0.60	572898.27	0.64	511835	0.57	297920	0.33
wizard of wor	563.5	<b>395300</b>	17862.5	4.38	9157.5	2.18	29059.3	7.22	26008	6.45
yars revenge	3092.9	<b>15000105</b>	102557	0.66	84231.14	0.54	166292.3	1.09	76903.5	0.49
zaxxon	32.5	<b>83700</b>	22209.5	26.51	32935.5	39.33	41118	49.11	46070.8	55.03
MEAN SABER(%)	0.00	<b>100.00</b>		28.39		29.45		36.78		50.11
MEDIAN SABER(%)	0.00	<b>100.00</b>		4.92		4.31		8.08		13.90



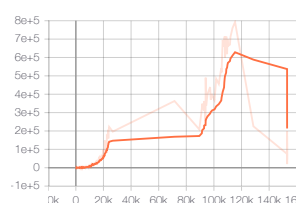
1. alien



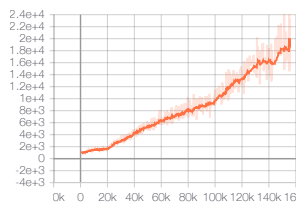
2. amidar



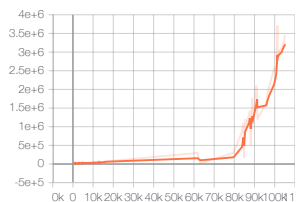
3. assault



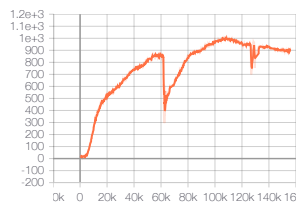
4. asterix



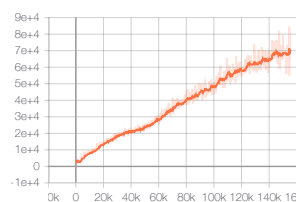
5. asteroids



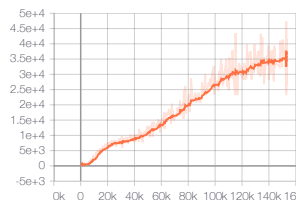
6. atlantis



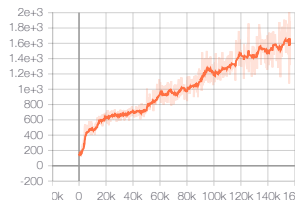
7. bank\_heist



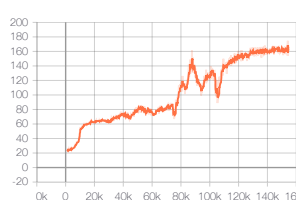
8. battle\_zone



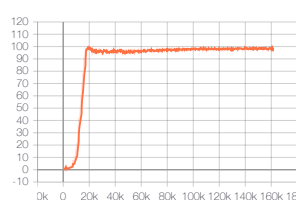
9. beam\_rider



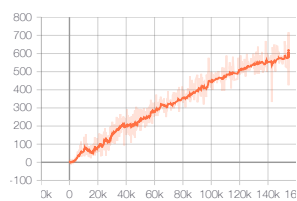
10. berzerk



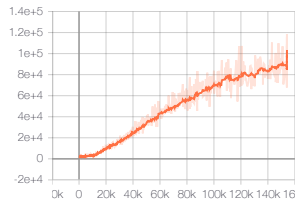
11. bowling



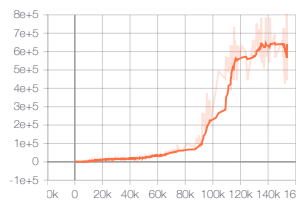
12. boxing



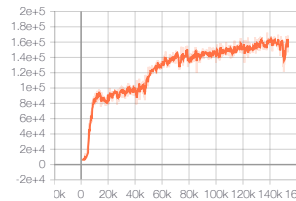
13. breakout



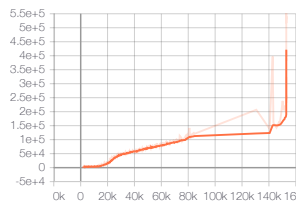
14. centipede



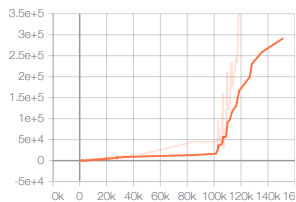
15. chopper\_command



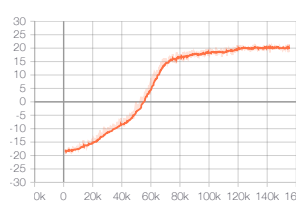
16. crazy\_climber



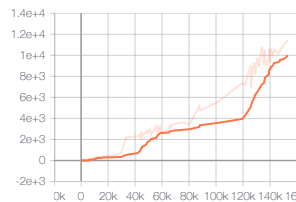
17. defender



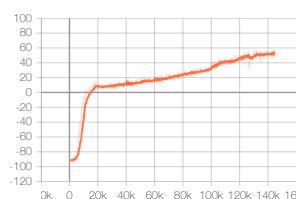
18. demon\_attack



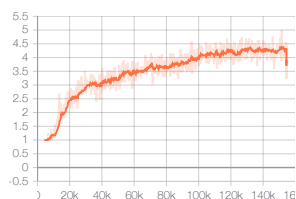
19. double\_dunk



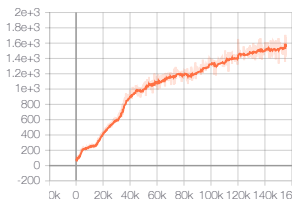
20. enduro



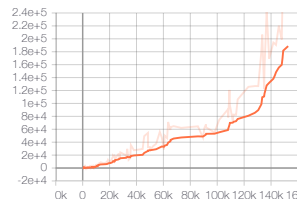
21. fishing\_derby



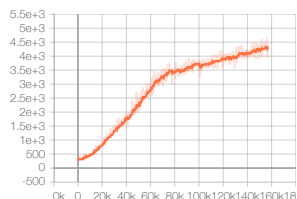
22. freeway



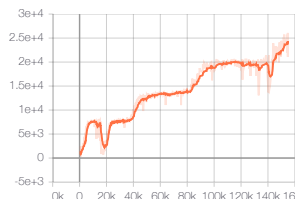
23. frostbite



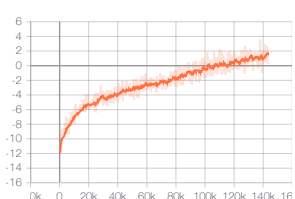
24. gopher



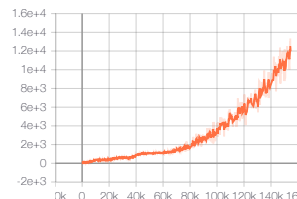
25. gravitar



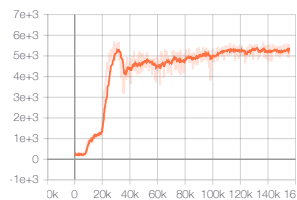
26. hero



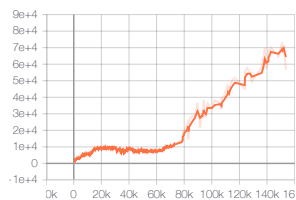
27. ice\_hockey



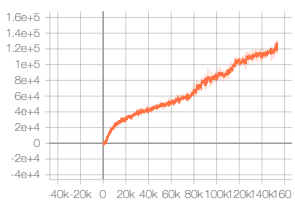
28. jamesbond



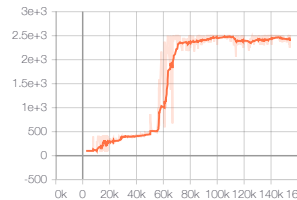
29. kangaroo



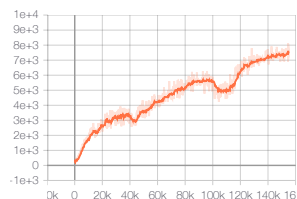
30. krull



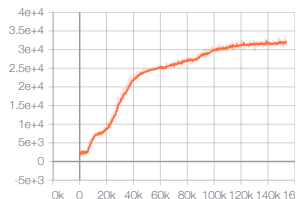
31. kung\_fu\_master



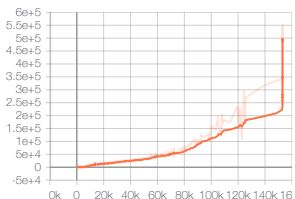
32. montezuma\_revenge



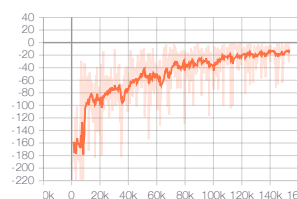
33. ms\_pacman



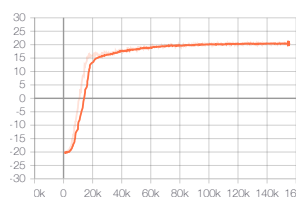
34. name\_this\_game



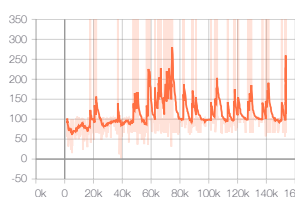
35. phoenix



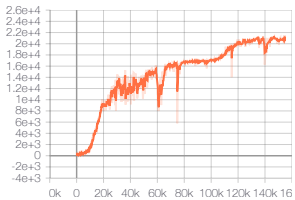
36. pitfall



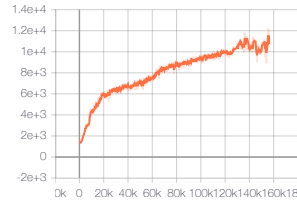
37. pong



38. private\_eye

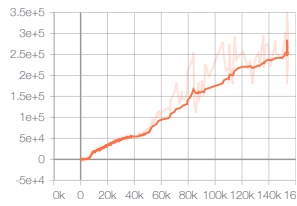


39. qbert

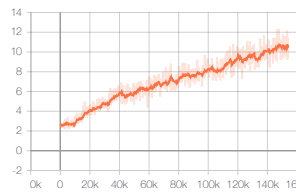


40. riverraid

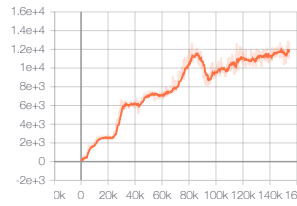




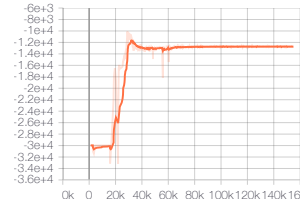
41. road\_runner



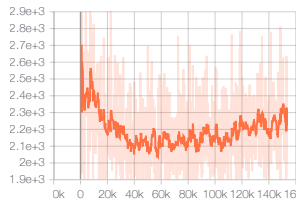
42. robotank



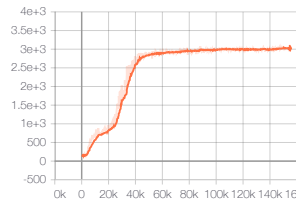
43. seaquest



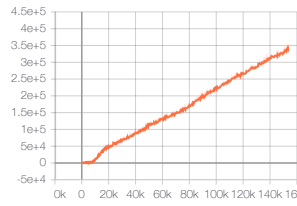
44. skiing



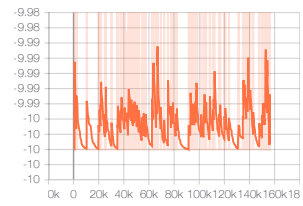
45. solaris



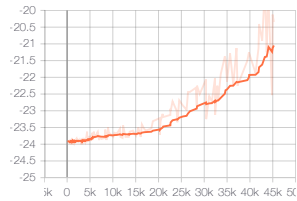
46. space\_invader



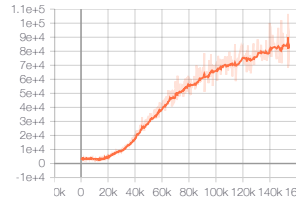
47. star\_gunner



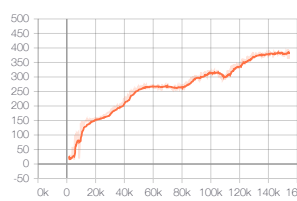
48. surround



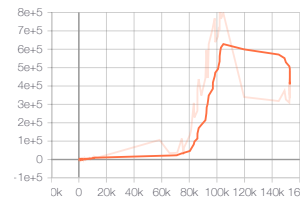
49. tennis



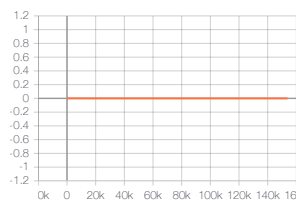
50. time\_pilot



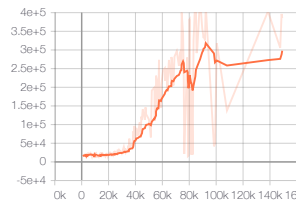
51. tutankham



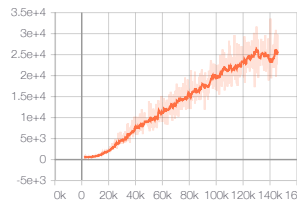
52. up\_n\_down



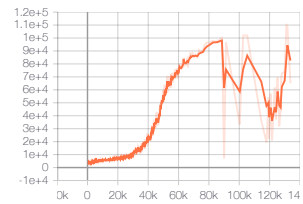
53. venture



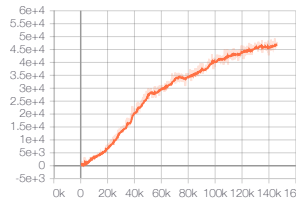
54. video\_pinball



55. wizard\_of\_wor



56. yars\_revenge



57. zaxxon